AIP | Applied Physics Letters

Magnetoresistance effects and spin-valve like behavior of an arrangement of two MnAs nanoclusters

M. Fischer, M. T. Elm, S. Sakita, S. Hara, and P. J. Klar

Citation: Applied Physics Letters **106**, 032401 (2015); doi: 10.1063/1.4906036
View online: http://dx.doi.org/10.1063/1.4906036
View Table of Contents: http://scitation.aip.org/content/aip/journal/apl/106/3?ver=pdfcov
Published by the AIP Publishing

Magnetoresistance effects and spin-valve like behavior of an arrangement of two MnAs nanoclusters

M. Fischer,[1] M. T. Elm,[1,2,a)] S. Sakita,[3] S. Hara,[3] and P. J. Klar[1]
[1]*Institute of Experimental Physics I, Justus-Liebig University, Heinrich-Buff-Ring 16, 35392 Giessen, Germany*
[2]*Institute of Physical Chemistry, Justus-Liebig University, Heinrich-Buff-Ring 58, 35392 Giessen, Germany*
[3]*Research Center for Integrated Quantum Electronics, Hokkaido University, North 13, West 8, Sapporo 060-8628, Japan*

(Received 28 November 2014; accepted 4 January 2015; published online 20 January 2015)

We report on magnetotransport measurements on a MnAs nanocluster arrangement consisting of two elongated single-domain clusters connected by a metal spacer. The arrangement was grown on GaAs(111)B-substrates by selective-area metal organic vapor phase epitaxy. Its structural properties were investigated using scanning-electron microscopy and atomic-force microscopy, while its magnetic domain structure was analyzed by magnetic-force microscopy. The magnetoresistance of the arrangement was investigated at 120 K for two measurement geometries with the magnetic field oriented in the sample plane. For both geometries, discrete jumps of the magnetoresistance of the MnAs nanocluster arrangement were observed. These jumps can be explained by magnetic-field induced switching of the relative orientation of the magnetizations of the two clusters which affects the spin-dependent scattering in the interface region between the clusters. For a magnetic field orientation parallel to the nanoclusters' elongation direction a spin-valve like behavior was observed, showing that ferromagnetic nanoclusters may be suitable building blocks for planar magnetoelectronic devices. © *2015 AIP Publishing LLC*. [http://dx.doi.org/10.1063/1.4906036]

Magnetoelectronic devices such as spin-valves consist in their simplest form of layered structures, where a thin diamagnetic or insulating layer is sandwiched between two ferromagnetic layers.[1] Their functionality is based on the giant magnetoresistance (GMR)[2,3] or tunneling magnetoresistance effect (TMR),[4] respectively, where spin-dependent scattering results in high or low resistance of the device depending on the relative magnetization orientation of the two magnetic layers.[5] Such magnetoelectronic devices are of huge interest for applications in the field of non-volatile memories, reading heads, or magnetic sensor devices.[6] Single spin-valves are mostly fabricated as layered structures in a stack-like geometry with well-defined magnetoresistance switching characteristics for fields in the plane of the layered system. In order to obtain a device such as a magnetic field sensor or angle-sensitive detector, usually, several of these layered spin-valves have to be connected to cover all three spatial directions.[7,8] Here, a planar device structure may offer an additional degree of freedom for the design of complex device structures. Additionally, planar structures can easily be integrated in magnetic non-volatile or domain wall memory devices, which also show a planar device structure.[9,10] Various spin-valve structures with different geometries based on, e.g., metals,[11,12] ferromagnetic (Ga,Mn)As alloys,[13–15] or Si nanowires[16] have been reported. Here, we present a different approach for planar magnetoelectronic devices using MnAs nanoclusters instead of ferromagnetic layers. The nanoclusters are grown self-assembled using selective-area metal organic vapor phase epitaxy (SA-MOVPE).[17,18] Besides a high structural quality, this method offers the possibility to precisely control the position of the nanoclusters as well as their size and shape.[18–20] The MnAs nanoclusters grown by SA-MOVPE show a magnetization orientation in the sample plane with an in-plane anisotropy which can be tuned by the clusters' shape.[19–21] These magnetic properties, a relatively high Curie-temperature of about 340 K (Refs. 22 and 23) as well as the advantage to control their position accurately make the MnAs nanoclusters grown by SA-MOVPE ideal building blocks for planar magneto-nanoelectronic device structures even for room temperature applications. Recently, theoretical calculations of the conductance through device structures consisting of MnAs nanoclusters predicted high magnetoresistance ratios of up to 300% due to spin-dependent scattering in the interface region between the single nanoclusters[24] supporting the idea that arrangements of MnAs nanoclusters are suitable building blocks for magnetoelectronic devices.

Scanning electron microscopy (SEM) images of the MnAs nanocluster arrangement investigated are shown in Figures 1(a) and 1(b). The arrangement consists of two separated nanoclusters with a gap of about 10 nm, whose elongation directions are preferably oriented parallel to each other and which are connected by a gold layer resulting in a planar GMR-like device structure. The longer cluster has a length of about 950 nm, while the shorter one is approximately 600 nm long. Figure 1(c) shows as an example a magnetic force microscopy (MFM) image of a nanocluster arrangement comparable to the GMR-like arrangement investigated. The two elongated nanoclusters are also separated by a small gap of 10 nm. Both nanoclusters form separated, single magnetic domains with the magnetization direction oriented parallel to the elongation direction of the nanoclusters. Figure 1(d) depicts the transmission electron microscopy image of a comparable arrangement of two MnAs clusters. This side view clearly shows that the vertical interfaces between

a)matthias.elm@exp1.physik.uni-giessen.de

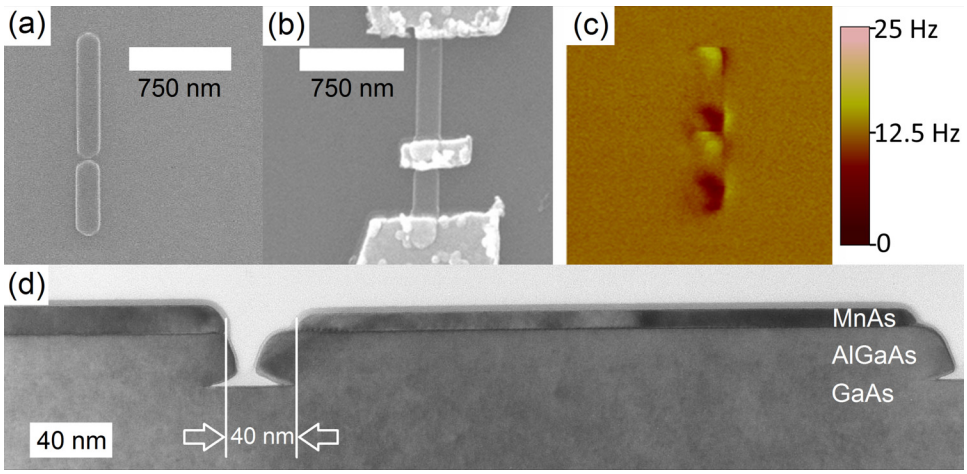

FIG. 1. (a) Scanning electron microscopy image of the investigated arrangement consisting of two MnAs nanoclusters with a gap of approximately 10 nm between them. (b) SEM image of the same arrangement connected by a gold strip. (c) Magnetic force microscopy image of an arrangement comparable to the investigated structure showing two single magnetic domains. (d) Transmission electron microscopy image of a comparable MnAs cluster arrangement with a larger gap of about 40 nm. GaAs substrate, AlGaAs buffer layer, and MnAs cluster are clearly visible.

GaAs, AlGaAs, and MnAs as well as the corresponding thicknesses of the three materials can be accurately controlled. The gap between the clusters which is filled with Au when the device structure is fabricated is also well defined, but harder to control in the fabrication process. In case of the structure shown in Fig. 1(d), the gap between the clusters is about 40 nm; in the device structure, it is about 10 nm.

The magnetic field dependence of the overall resistance of the nanocluster arrangement consists of two magnetoresistance contributions. First, a large linear magnetoresistance of about 10% is found at high magnetic fields of 10 T. The large linear MR is the consequence of the existence of a parallel transport path through the substrate. During the growth of the nanoclusters, Mn diffuses into the substrate resulting in a p-type doped GaAs:Mn matrix.[26,27] The current path through the p-type matrix yields a large linear MR effect, which is typically for granular MnAs/GaAs:Mn hybrid structures.[25] Furthermore, the overall magnetoresistance exhibits abrupt jumps of the resistance which can be observed at about 2 to 3 T. The magnetoresistance changes abruptly by 1%–2%. We relate this effect to magnetization switching in the external magnetic field. In order to provide a better visibility of the resistance jumps caused by the magnetization switching, the large linear MR was subtracted from the measured resistance.

Figure 2(a) shows the background-subtracted magnetoresistance of the GMR-like arrangement for a magnetic field sweeping in-plane and with its direction parallel to the nanoclusters' elongation direction. For this measurement geometry, the MR behavior is that expected of a spin-valve device, where one jump of the resistance for each sweeping direction can be observed. The first jump occurs at −1.0 T on the upsweep (black triangles), while a second jump is observed at −3.1 T on the downsweep (red squares). For a different field geometry, where the magnetic field orientation is in-plane and perpendicular to the elongation direction of the

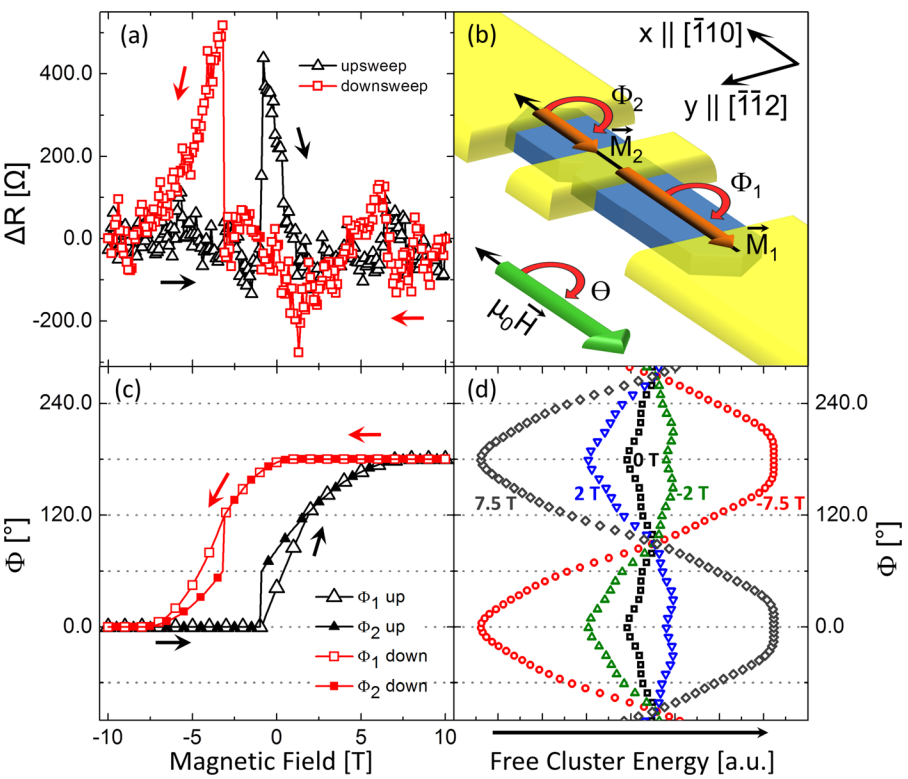

FIG. 2. (a) Behavior of the background-subtracted magnetoresistance of the nanocluster arrangement for the magnetic field direction parallel to the elongation direction of the nanoclusters. (b) Schematic illustration of the nanocluster device defining the angles Φ_1, Φ_2, and Θ. (c) Variations of the magnetization orientations of the nanoclusters expressed in terms of Φ_1 and Φ_2. (d) Energy landscapes of the magnetization of an elongated MnAs nanocluster at different external magnetic fields as a function of Φ_i.

nanoclusters, only one abrupt change of the resistance can be observed as shown in Figure 3(a). The jump occurs at −2.4 T on the upsweep. After each jump, one observes a continuous decrease of the MR back to its original value.

The jumps in the magnetoresistance may be explained by changes of the relative angle between the magnetizations of the two clusters and the resulting spin-dependent scattering in the interface region between the two nanoclusters.[24] It is therefore necessary to evaluate the magnetization orientation of both nanoclusters by minimizing the free energy of the corresponding nanocluster arrangement. Because the nanoclusters show a hard magnetic axis along the *c*-direction,[26] the clusters' magnetizations are assumed to be oriented in the sample plane. In the sample plane, the MnAs nanoclusters exhibit a magnetocrystalline anisotropy contribution with a six-fold symmetry and an additional shape anisotropy with a 180° symmetry, due to the elongation of the nanoclusters.[27,30] Because of the small separation of the nanoclusters, coupling of the individual magnetic domains has to be considered. This coupling can be described by a Heisenberg coupling term. The total free energy of the system in an external magnetic field can therefore be described as follows:[28,29]

$$\begin{aligned} U_{tot} = & -JM_1M_2\cos(\Phi_1 - \Phi_2) \\ & + \sum_{i=1}^{2}(-\mu_0 M_i H V_i \cos(\Phi_i - \Theta) \\ & + K_i V_i \sin^2(\Phi_i - \varepsilon_i) + K_4 V_i \cos(6\Phi_i)). \end{aligned} \quad (1)$$

Here, J is the coupling constant of the Heisenberg-like coupling between the magnetizations M_1 and M_2 of the two clusters and Φ_1 and Φ_2 are the corresponding angles of the magnetization directions in the sample plane with respect to the elongation direction of the nanoclusters, i.e., the $[\bar{1}10]$-direction of the substrate. V_i are the volumes of the clusters, H is the external magnetic field, Θ is the angle of the external magnetic field with respect to the $[\bar{1}10]$-direction, μ_0 is the magnetic permeability in vacuum, K_i and ε_i are the shape anisotropy constants and the elongation directions of the corresponding nanoclusters, respectively, and K_4 is the magnetocrystalline anisotropy constant. The definition of the angles for each measurement geometry is shown in Figures 2(b) and 3(b). For the interpretation of the discrete jumps of the resistance, the energy density landscapes of the individual magnetizations M_1 and M_2 of the coupled cluster system were analyzed qualitatively to evaluate the magnetization orientation of each cluster with sweeping external magnetic field. A schematic illustration of the corresponding magnetization orientations (characterized by the angles Φ_1 and Φ_2) explaining the observed changes in the resistance are shown in Figures 2(c) and 3(c), while the corresponding energy landscapes for one of the magnetizations M_i at selected external magnetic field strengths are shown in Figures 2(d) and 3(d).

For the case shown in Figure 2, where an external magnetic field was applied parallel to the elongation direction of the nanoclusters, the changes in the resistance can be explained as follows: At high positive magnetic fields, the energy landscape shows a global minimum at $\Phi = 180°$ due to the Zeeman energy contribution for a magnetic field strength of 7.5 T as shown in Figure 2(d). Thus, the magnetizations Φ_i of both nanoclusters are oriented parallel to the external field direction ($\Phi_1 = \Phi_2 = 180°$, red squares in Figure 2(b)), i.e., they are aligned parallel to each other resulting in low spin-dependent scattering. Because the external magnetic field is applied parallel to the elongation direction of the clusters, where the energy landscape shows a minimum due to the nanoclusters' shape anisotropy even in

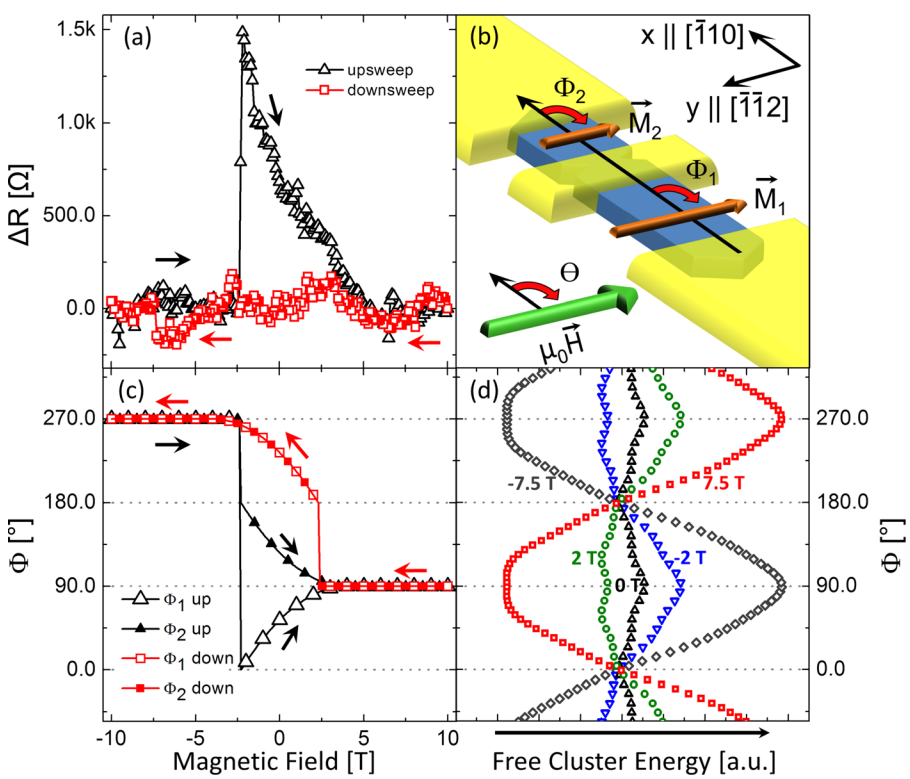

FIG. 3. (a) Behavior of the background-subtracted magnetoresistance of the nanocluster arrangement for the magnetic field direction perpendicular to the elongation direction of the nanoclusters. (b) Schematic illustration of the nanocluster device defining the angles Φ_1, Φ_2, and Θ. (c) Variations of the magnetization orientations of the nanoclusters expressed in terms of Φ_1 and Φ_2. (d) Energy landscapes of the magnetization of an elongated MnAs nanocluster at different external magnetic fields as a function of Φ_i.

the absence of an external field (the corresponding energy landscape is shown in Figure 2(d) as black squares), the magnetization orientation will not change with decreasing field strength in agreement with the experimental observation on the downsweep. Both magnetization angles Φ_i will therefore remain at $\Phi = 180^\circ$ for a decreasing field. Changing the field polarity from $\Theta = 0^\circ$ to 180° and increasing the magnetic field strength again the Zeeman energy contribution will cause a global minimum at $\Phi_i = 0^\circ$ favoring the opposite magnetization orientation. As can be seen in the energy landscape for a magnetic field of $-2\,\mathrm{T}$ shown in Figure 2(d), with increasing negative magnetic field the minimum at 180° starts to vanish. Therefore, both magnetizations will slowly start to rotate towards the external field direction leading to decreasing magnetization angles Φ_i. At a certain field value, the magnetization of the smaller nanocluster may jump abruptly towards the magnetic easy axis at $\Phi = 60^\circ$ which is closer to the external magnetic field direction, while the magnetization of the longer cluster will keep rotating continuously towards the external field direction due to its stronger shape anisotropy compared to the smaller one. Because the magnetizations of the two nanoclusters are not oriented parallel anymore as illustrated in Figure 2(b), spin-dependent scattering in the interface region increases leading to an abrupt jump of the resistance. Increasing the magnetic field further, the magnetizations of both clusters continuously rotate towards $\Phi = 0^\circ$, i.e., parallel to the external field direction, resulting in a continuous decrease of spin scattering and therefore in a decreasing magnetoresistance. At high negative fields, both clusters are oriented parallel to the external field direction again. For both sweeping directions of the external field, one observes a similar behavior. Altogether, the planar GMR-like arrangement shows a behavior which is somewhat similar to a spin-valve device. Interestingly, the observed switching of the magnetization orientations does occur at different external field strengths for the two sweeping directions. On the upsweep, the magnetization jump is observed even before the polarity change of the external field. This behavior may be caused by the thermal activation of rotations of the magnetizations, which are not taken into account in the model. At low magnetic fields and a temperature of 120 K, where the measurements were performed, the thermal energy may be sufficient to overcome the energy barriers in the energy landscape of the nanoclusters, which arise due to the magnetocrystalline and shape anisotropy. Thus, the magnetization may jump spontaneously into another energy minimum even before the polarity of the magnetic field changes, which explains the abrupt changes of the resistance. Thus, for a quantitative description of the observed magnetoresistance behavior at 120 K, thermal effects have to be taken into account.

Using the same model, we also performed an analysis of the results for the other measurement geometry, where the magnetic field is oriented perpendicular to the elongation direction of the nanoclusters. As can be seen in Figure 3(a), a resistance jump is observed for this measurement geometry only on the upsweep, but not on the downsweep. This behavior is due to the fact that for this geometry, the minima in the energy landscape due to Zeeman energy contribution are now located at $\Phi_i = 90^\circ$ or 270° and therefore shifted by 90° with respect to the minima of the energy landscape caused by the shape anisotropy of the nanoclusters at $\Phi_i = 0^\circ$ and 180°, which dominate the magnetic behavior at low fields. Thus, in contrast to the parallel geometry, the global minimum in the energy landscape of the magnetization at high positive fields (at $\Phi_i = 90^\circ$) becomes a maximum at low fields; simultaneously, two almost equivalent minima arise at $\Phi_i = 0^\circ$ and 180°, respectively. Assuming thermal activation and only a small coupling between the clusters' magnetizations, the probability for the magnetizations to end up in a parallel orientation (e.g., $\Phi_1 = \Phi_2 = 180^\circ$ or in an antiparallel orientation (e.g., $\Phi_1 = 0^\circ$ and $\Phi_2 = 180^\circ$) are almost the same. At high positive magnetic fields, the magnetization of both clusters is aligned parallel to the external magnetic field, i.e., $\Phi_i = 90^\circ$ and thus perpendicular to the elongation direction of the clusters. With the decrease in magnetic field, the Zeeman energy contribution weakens and a magnetization alignment parallel to the nanoclusters' elongation direction at either $\Phi_i = 0^\circ$ or $\Phi_i = 180^\circ$ is more favorable, resulting in abrupt jumps of the magnetizations. This consideration is the basis of the explanation of the magnetoresistance behavior observed in Figure 3(a). On the downsweep, no jump of the magnetoresistance is observed because with the decrease in external field, the magnetizations of the clusters jump into a parallel alignment, e.g., $\Phi_1 = \Phi_2 = 180^\circ$ as shown in Figure 3(c) (red squares). Thus, no spin-dependent scattering occurs, and therefore, no change of the resistance is observed. On the upsweep, the nanoclusters' magnetizations jump into an antiparallel alignment, i.e., the magnetizations are oriented along the elongation direction of the nanoclusters but along opposite directions, e.g., $\Phi_1 = 0^\circ$ and $\Phi_2 = 180^\circ$ as shown in Figure 3(c) (black triangles). The antiparallel alignment results in strong spin-dependent scattering between the clusters and therefore in a larger resistance. With the increase in negative field, the magnetizations slowly rotate towards an orientation parallel to the external magnetic field direction resulting in a continuous decrease of the resistance until both magnetizations are finally oriented parallel to the external magnetic field direction. However, as pointed out above, in this geometry, the behavior of the magnetizations on the up- and downsweeps is hardly predictable as the magnetization jumps at low fields towards a parallel alignment ($\Phi_1 = \Phi_2 = 0^\circ$ or $\Phi_1 = \Phi_2 = 180^\circ$) or antiparallel alignment ($\Phi_1 = 0^\circ$ and $\Phi_2 = 180^\circ$ or vice versa) occur with similar probabilities. The former shows no magnetoresistance jump, the latter does. Thus, the magnetoresistance behavior shows a certain degree of randomness.

In summary, we demonstrated the preparation of a planar, GMR-like nanocluster arrangement for possible magnetoelectronic device applications. The arrangement prepared by SA-MOVPE consists of elongated nanoclusters which exhibit a magnetization orientation along their elongation direction in the absence of an external magnetic field. At 120 K, the magnetoresistance of the arrangement shows abrupt jumps, which can be explained by spin-dependent scattering at the clusters' interface region caused by changes of the relative angle between the magnetization directions of the two clusters due to the applied external magnetic field, but also due to thermally activated rotation of the magnetization. For an external magnetic field direction applied parallel

to the elongation direction of the nanoclusters, the magnetoresistance exhibits a well defined behavior similar to a spin-valve device. However, in case of the field geometry, where the magnetic field is applied perpendicular to the nanoclusters' elongation direction, the interplay of the Zeeman effect and the shape anisotropy introduces a certain degree of randomness in the switching behavior of the magnetoresistance of the nanocluster arrangement. The magnetoresistance effect due to the magnetization switching of about 1–2% appears to be comparatively small. However, one has to keep in mind that a large contribution to the overall resistance arises from shunt currents through the substrate, which reduces the relative MR related to the switching. Additionally, the relatively large gap of 10 nm between the two clusters filled with Au is not optimal for achieving large MR effects. Thus, a significant increase of the effect may be achieved by improving the insulation between nanocluster and substrate and by reducing the gap between the clusters. Nevertheless, these results show that MnAs nanoclusters possess the potential to serve as building blocks for planar magneto-nanoelectronic devices. As position and shape of the nanoclusters can be accurately controlled very complex in-plane device structures may be anticipated. By adjusting the aspect ratio and thus the in-plane magnetic anisotropy of the nanoclusters, it should be possible to tune the switching characteristics of such arrangements. However, to achieve such reliable device characteristics, further investigations are needed, in particular, the influence of temperature on thermally activated magnetization rotations and the resulting changes in the resistance need to be studied in detail.

The authors thank DFG, DAAD, and JSPS for financial support.

[1]G. A. Prinz, Science **282**, 1660 (1998).
[2]G. Binasch, P. Gruenberg, F. Saurenbach, and W. Zinn, Phys. Rev. B **39**, 4828 (1989).
[3]P. Gruenberg, R. Schreiber, Y. Pang, M. B. Brodsky, and H. Sowers, Phys. Rev. Lett. **57**, 2442 (1986).
[4]M. Julliere, Phys. Lett. A **54**, 225 (1975).
[5]S. S. P. Parkin, Annu. Rev. Mater. Sci. **25**, 357 (1995).
[6]S. A. Wolf, D. D. Awschalom, R. A. Buhrman, J. M. Daughton, S. von Molnár, M. L. Roukes, A. Y. Chtchelkanova, and D. M. Treger, Science **294**, 1488 (2001).
[7]C. Reig, M.-D. Cubells-Beltran, and D. Ramirez Munoz, Sensors **9**, 7919 (2009).
[8]R. Weiss, R. Mattheis, and G. Reiss, Meas. Sci. Technol. **24**, 082001 (2013).
[9]S. S. P. Parkin, M. Hayashi, and L. Thomas, Science **320**, 190 (2008).
[10]D. A. Allwood, G. Xiong, M. D. Cooke, C. C. Faulkner, D. Atkinson, N. Vernier, and R. P. Cowburn, Science **296**, 2003 (2002).
[11]M. Johnson and R. H. Silsbee, Phys. Rev. Lett. **55**, 1790 (1985).
[12]Y. Manzke, R. Farshchi, P. Bruski, J. Herfort, and M. Ramsteiner, Phys. Rev. B **87**, 134415 (2013).
[13]K. F. Eid, L. E. Ocola, X. Liu, and J. K. Furdyna, Appl. Phys. Lett. **102**, 242407 (2013).
[14]K. Pappert, S. Huempfner, C. Gould, J. Wenisch, K. Brunner, G. Schmidt, and L. W. Molenkamp, Nat. Phys. **3**, 573 (2007).
[15]A. D. Giddings, M. N. Khalid, T. Jungwirth, J. Wunderlich, S. Yasin, R. P. Campion, K. Edmonds, J. Sinova, K. Ito, K. Y. Wang, D. Williams, B. L. Gallagher, and C. T. Foxon, Phys. Rev. Lett. **94**, 127202 (2005).
[16]J. Tarun, S. Huang, Y. Fukuma, H. Idzuchi, Y. Otani, N. Fukata, K. Ishibashi, and S. Oda, J. Appl. Phys. **109**, 07C508 (2011).
[17]S. Hara, D. Kawamura, H. Iguchi, J. Motohisa, and T. Fukui, J. Cryst. Growth **310**, 2390 (2008).
[18]T. Wakatsuki, S. Hara, S. Ito, D. Kawamura, and T. Fukui, Jpn. J. Appl. Phys., Part 2 **48**, 04C137 (2009).
[19]S. Ito, S. Hara, T. Wakatsuki, and T. Fukui, Appl. Phys. Lett. **94**, 243117 (2009).
[20]K. Komagata, S. Hara, S. Ito, and T. Fukui, Jpn. J. Appl. Phys. **50**, 06GH01 (2011).
[21]M. T. Elm, P. J. Klar, S. Ito, S. Hara, and H.-A. Krug von Nidda, Phys. Rev. B **84**, 035309 (2011).
[22]T. Hartmann, M. Lampalzer, P. J. Klar, W. Stolz, W. Heimbrodt, H.-A. Krug von Nidda, A. Loidl, and L. Svistov, Physica E **13**, 572 (2002).
[23]H.-A. Krug von Nidda, T. Kurz, A. Loidl, T. Hartmann, P. J. Klar, W. Heimbrodt, M. Lampalzer, K. Volz, and W. Stolz, J. Phys.: Condens. Matter **18**, 6071 (2006).
[24]C. Heiliger, M. Czerner, P. J. Klar, and S. Hara, IEEE Trans. Magn. **46**, 1702 (2010).
[25]S. Ye, P. J. Klar, T. Hartmann, W. Heimbrodt, M. Lampalzer, S. Nau, T. Torunski, W. Stolz, T. Kurz, H.-A. Krug von Nidda, and A. Loidl, Appl. Phys. Lett. **83**, 3927 (2003).
[26]M. T. Elm, C. Michel, J. Stehr, D. M. Hofmann, P. J. Klar, S. Ito, S. Hara, and H.-A. Krug von Nidda, J. Appl. Phys. **107**, 013701 (2010).
[27]M. T. Elm, P. J. Klar, S. Ito, and S. Hara, Phys. Rev. B **83**, 235305 (2011).
[28]A. Thiaville, J. Magn. Magn. Mater. **182**, 5 (1998).
[29]M. Labrune, J. Kools, and A. Thiaville, J. Magn. Magn. Mater. **171**, 1 (1997).
[30]S. Hara and T. Fukui, Appl. Phys. Lett. **89**, 113111 (2006).